Received: 15 Nov 2024 | Revised: 24 Mar 2025 | Accepted: 05 May 2025 | Published: 20 May 2025
Volume 3(1) Pages 63-74
DOI: https://doi.org/ 10.56279/jicts.v3i1.155

JICTS
Journal of ICT Systems

Hybrid Dehazing Algorithm for Enhancing Quality of Homogeneous and Non-Homogeneous Hazy Images

Easter Christopher, Josiah Nombo, Nassor Ally[1]

Department of Electronics and Telecommunications Engineering, University of Dar Es Salaam, Dar Es Salaam, Tanzania

[1]Corresponding author
Email: nassorkindy@gmail.com

Funding information

This work was self-funded.

Abstract

Restoring high-quality images from hazy environments presents a significant challenge, particularly when dealing with both homogeneous and non-homogeneous haze images. Homogeneous haze is uniformly distributed, while non-homogeneous haze varies across the image, making it difficult for existing dehazing methods to balance image clarity, preserve fine details, and minimize artifacts, such as color distortion. To address these challenges, this study proposes a hybrid dehazing algorithm that integrates fusion-based techniques with Dark Channel Prior (DCP) and guided filtering to enhance atmospheric light estimation and refine the transmission map. A multi-scale fusion process is then applied to recover scene radiance, enhancing visual quality. Performance tests on standard datasets, including RESIDE and NH-HAZE, demonstrate the algorithm's effectiveness, outperforming other state-of-the-art methods, achieving an average Peak Signal-to-Noise Ratio (PSNR) of 26.70 dB and an average Structural Similarity Index Measure (SSIM) of 0.8843. These results underscore the algorithm's effectiveness in improving image quality while maintaining computational efficiency.

Keywords

Fusion-Based Method
Hybrid Algorithm
Image Dehazing
Homogeneous haze Non-Homogeneous Haze

1. Introduction

1.1 Background

Images play a crucial role in how we process and retain information. Research suggests visuals are more engaging and memorable than text-based content [1]. Images captured outdoors, however, face unique challenges due to environmental factors, particularly haze, which obscures visibility by scattering light particles in the atmosphere [2]. Haze can be either homogeneous, uniformly affecting the image, or non-homogeneous, creating uneven distortion across different regions [3]. This interference reduces image quality, clarity, and contrast. This problem restricts images to be used in applications requiring high clarity and accuracy, such as weather forecast activities and environmental monitoring [4].

Image dehazing, or haze removal, restores clear visuals from hazy images using techniques that have evolved from basic contrast adjustments to sophisticated models based on atmospheric scattering and deep learning [5]. Deep learning methods, such as those proposed by Zhang et al. [12] and Zhou [17], excel at detecting and removing haze, but often require high computational power, limiting their accessibility in regions with inadequate technological resources [6-8]. Additionally, deep learning-based methods produce inconsistent results across different environments due to data variations, underscoring the need for alternative methods that provide flexibility and generalization [9].

To address these challenges, fusion-based methods are deployed, combining the strengths of multiple approaches to enhance dehazing effectiveness while maintaining computational efficiency [3]. Fusion methods use multi-layered processing to retain significant image features. For instance, work discussed by Dehazing et al. [5] known as joint contrast enhancement and exposure fusion (CEEF) frameworks has demonstrated promising results in improving visibility under non-uniform haze conditions, offering a balanced approach that integrates deep learning efficiency with conventional methods' reliability.

Despite these advances, a notable gap persists: developing algorithms that can effectively handle both homogeneous and non-homogeneous haze [11, 12]. Most existing techniques excel in either homogeneous or non-homogeneous scenarios, but rarely perform well under both imaging conditions [13]. Non-homogeneous haze remains particularly challenging due to its variable intensity, which complicates the dehazing process [13]. This study aims to bridge this gap by proposing a novel hybrid fusion-based algorithm that integrates the Dark Channel Prior (DCP) method with additional image processing. Our method effectively tackles haze in both homogeneous and non-homogeneous images while keeping the algorithm unchanged. The system initially classifies the image as homogeneous or non-homogeneous, then executes the relevant code section for dehazing. This approach provides a practical and computationally efficient solution, improving dehazing quality for a range of real-world applications.

As image processing techniques develop, the approach to image dehazing also evolves [6]. Initially, the image dehazing problem was treated as an image enhancement problem, using algorithms such as contrast enhancement and Retinex for defogging based on human perception. Later, image restoration methods based on the atmospheric scattering model were developed to solve the image dehazing problem. It involved mathematical techniques to recover the original image. Due to the complexity of the image dehazing problem, fusion-based solutions were developed as a result of researchers combining multiple methods into one to improve performance [3]. Recently, with the advancement of deep learning technology, the emergence of deep learning has revolutionized the field of image dehazing, leading to significant improvements in dehazing performance [7]. It extracts the deep features of a hazy image through a convolutional neural network to find the mapping between hazy and clear images, proving superiority in robustness and performance.

However, deep learning methods for image dehazing often require complex mathematical models and significant computational power, particularly high-performance GPUs which contribute to long processing times [3]. This complexity makes them challenging to implement in resource-limited setting [5]. Due to these limitations, fusion-based methods have emerged as a more practical alternative, offering simplicity and computation efficiency. By combining multiple techniques, fusion-based methods produce higher quality dehazed images. Moreover, Dark Channel Prior (DCP) with guided filtering-based approaches have shown competitive results when compared to other state-of-the-art methods.

1.2 Related Theory

In image processing, the atmospheric scattering model widely used to describe the formation of haze in images [8] is as follows:

$$I(x) = J(x)t(x) + A\big(1 - t(x)\big) \quad (1)$$

where x is the pixel's location, I is the observed intensity, J is the scene radiance, A is the global atmospheric light, and t is the medium transmission. The goal of haze removal is to recover J, A, and t from $I(x)$. Equation (2) is used to achieve this.

$$I(x) - A = \max(t(x), t_o)\,(J(x) - A) \quad (2)$$

The difficulty in recovering image J lies in that both t and A parameters are unknown. A useful tool for computing the unknown variables is presented: the dark channel (DC). The DC is defined as follows:

$$J_{dark}(x) = min_{c\in\{r,g,b\}}\left(min_{y\in\Omega(x)}\big(J^c(y)\big)\right) \quad (3)$$

J^c is a color channel of J, and Ω(x) is a local patch centred at x and $cg\{r, g, b\}$ is intensity of the RGB image. Dividing equation (1) by A gives

$$min_{y\in\Omega(x)}\left(\frac{I^c(y)}{A^c}\right) = \tilde{t}(x) min_{y\in\Omega(x)}\left(\frac{J^c(x)}{A^c}\right) + \big(1 - \tilde{t}(x)\big) \quad (4)$$

Taking the min (·) operation among three color channels on equation (4), we obtain:

$$min_{c\in\{r,g,b\}}\left[min_{y\in\Omega(x)}\left(\frac{I^c(y)}{A^c}\right)\right] = \tilde{t}(x) min_{c\epsilon\{r,g,b\}}\left[min_{y\in\Omega(x)}\left(\frac{J^c(x)}{A^c}\right)\right] + \big(1 - \tilde{t}(x)\big) \quad (5)$$

According to the dark channel prior, the dark channel J^{dark} of the haze-free radiance J should tend to be zero:

$$J_{dark}(x) = min_{c\in\{r,g,b\}}\left(min_{y\in\Omega(x)}\big(J^c(y)\big)\right) = 0 \quad (6)$$

As A^c is always positive, this leads to

$$min_{c\in\{r,g,b\}}\left[min_{y\in\Omega(x)}\left(\frac{J^c(x)}{A^c}\right)\right] = 0 \quad (7)$$

Putting equation (3) into (4), we can estimate the transmission t simply as

$$\tilde{t}(x) = 1 - min_{c\in\{r,g,b\}}\left[min_{y\in\Omega(x)}\left(\frac{J^c(x)}{A^c}\right)\right] \quad (8)$$

We introduce a constant parameter ω (0<ω<1) into Equation (8), which can keep a very small amount of haze for the distant objects;

$$\tilde{t}(x) = 1 - \omega min_{c\in\{r,g,b\}}\left[min_{y\in\Omega(x)}\left(\frac{J^c(x)}{A^c}\right)\right] \quad (9)$$

The parameter ω ∈ [0,1] is empirically chosen to 0.95 to substantially lower the transmission map and prevent over-enhancement. This value, first proposed by He et el. [9], strikes an appropriate balance between haze removal and natural image appearance. Subsequent study has confirmed this decision. Lee et al. [10] examined the influence of several ω values and found that ω about 0.9 efficiently reduces transmission map and improves visual quality. Setting ω to 0.95 achieves a good mix between removing haze and preserving image quality.

A^c is considered constant in all the images and is estimated by first selecting the 0.01% of the map generated when the dark channel is computed, $I^c(y)$ is the intensity of pixel y in the color channel c, $\Omega(x)$ is a local patch centered at x.

With the transmission map, we can recover the scene radiance J according to Equation (1) and Equation (3). The directly recovered scene radiance is prone to noise. Therefore, we restrict the transmission $t(x)$ to a lower bound t_o, which means that a certain small amount of haze is preserved in very dense haze regions.

1.3 Related Work

Recent studies on image dehazing have explored various methods to address the challenges of effective haze removal [11]. Zhang et al. [12] introduced a deep learning-based method with a hierarchical feature fusion network using mixed convolution attention to capture both global and local haze features, offering clearer, detailed images, but faced high computational costs and issues with non-homogeneous haze. Liu et al. [13] developed a fast, multi-scale patch-based fusion framework that avoids relying on atmospheric models, using contrast enhancement and exposure fusion (CEEF) to improve local visibility and global contrast. While it outperforms methods in homogeneous haze conditions, it struggles with non-homogeneous haze. Huang et al. [14] proposed a haze removal method using histogram gradient feature guidance (HGFG), which focused on pixel intensity histograms to preserve edges and improve contrast, offering superior performance to traditional methods but struggling with low-contrast images and requiring precise parameter tuning.

Despite significant advancements in image dehazing, existing methods struggle with non-homogeneous haze, often leading to image quality loss and underperformance in critical applications. Models designed for homogeneous haze fail in non-homogeneous conditions, and vice versa. This study proposes a fusion-based algorithm that effectively addresses both types of haze, ensuring high-quality, artefact-free images suitable for various computer vision tasks, without compromising computation efficiency. By integrating existing techniques, the algorithm offers an adaptive, efficient solution for haze removal.

2. Method

2.1 Proposed Method

The dehazing process involves multiple stages, starting with two input images: hazy image $I(x)$ and ground truth $G(x)$, both resized by 50%. Atmospheric light A is estimated from the dark channel of the resized hazy image:

$$A = mean\big(I(x_i)\big) \text{ for } I(x_i) \in T \tag{10}$$

Where T is the set of pixels with the highest values in the dark channel.

The Dark Channel Prior method was applied to estimate haze in the image. The dark channel $D(x)$ is defined as:

$$D(x) = min_{y\in\Omega(x)}\left(min_{c\in\{r,g,b\}}\big(I^c(y)\big)\right) \tag{11}$$

where $\Omega(x)$ is a local patch centered at x, $I^c(y)$ is the intensity of pixel y in the color channel c

Next, the Transmission Map $t(x)$ was computed as:

$$t(x) = 1 - \omega D(x) \tag{12}$$

where: ω is a parameter that controls the amount of haze to be removed (usually close to 1).

Then, the Refined Transmission map was refined

as $t_{refined}(x)$ using a guided filter:

$$t_{refined}(x) = GuidedFilter(t(x), I(x), patchSize, \lambda) \tag{13}$$

$$t_{refined}(x) = \frac{\sum_{y\epsilon\Omega}\big((I(x)-\mu_I)(t(y)-\mu_t)\big)}{\sigma_I^2+\epsilon} \tag{14}$$

where: μ_I and μ_t are the means of the image and the transmission map in a local patch, σ^2 is the variance of the image patch, ϵ is a regularization term to prevent division by zero. Here, guided filter applies a local smoothing operation to the transmission map based on the hazy image.

Scene radiance $J(x)$ is then recovered:

$$J(x) = \frac{I(x)-A}{\max\,(t(x),t_{o})} + A \quad (15)$$

Post-processing steps, such as Gaussian Filtering,

Contrast Limited Adaptive Histogram Equalization (CLAHE), Gamma Correction and White Balance were applied to refine the image. Gaussian filtering is applied to smooth the scene radiance and reduce noise.

$$J_{filtered}(x) = \frac{1}{2\pi\sigma^2}\sum_y \exp\left(-\frac{|x-y|^2}{2\sigma^2}\right) J(x) \quad (16)$$

where σ is the standard deviation of the Gaussian filter, $|x-y|^2$ represents the squared distance between pixels, and the term $\sum_y \exp\left(-\frac{|x-y|^2}{2\sigma^2}\right)$ defines the Gaussian kernel. This kernel determines the weights based on the distance between the central pixel and its neighbors, with closer pixels receiving higher weights.

The Gaussian filter was chosen for its simplicity, computational efficiency, memory efficiency, and well-established haze removal performance, which provides the best balance of quality and cost

CLAHE is applied to enhance contrast.

$$J_{CLAHE=\sum_{K=0}^{L-1}\frac{n_k}{N}.I_{k(x)}} \quad (17)$$

where: L is the number of gray levels, n_k is the number of pixels with intensity k within the local tile, N is the total number of pixels. Gamma correction is applied for brightness adjustment:

$$J_{gamma}(x) = J_{CLAHE}^{\gamma}(x) \quad (18)$$

White Balance correction is then performed to ensure color accuracy by scaling the RGB (Red, Green, Blue) channels to neutralize color imbalances. This can be done using the gray world assumption

$$J_{white}(x) = Whitebalance\left(J_{gamma}(x)\right) \quad (19)$$

$$J_{white}^{c}(x) = J_{gamma}^{c}.\frac{\mu_{gray}}{\mu_c} \quad (20)$$

where: $J_{white}^{c}(x)$ is the corrected intensity in the channel c (either R, G, or B), $\mu gray$ is the average intensity across all channels (the "gray" intensity), μc is the mean intensity of the channel c.

After applying the above transformations,

the general equation for the final dehazed image is provided in equation (21).

$$J_{final} = CLAHE\left(GC\left(GF\left(\frac{hazyImage - A}{\max(1-\omega.darkchannel, t_o)} + A, \sigma_{gausian}\right), \gamma_{value}\right), ClipLimit, Distribution\right) \quad (21)$$

where, $hazyImage$ is the input hazy image, A is the atmospheric light, which is estimated to assist in haze removal. $\omega.darkChannel$: Dark Channel Prior term used to estimate haze levels in an image, t_0: is the initial transmission map, $\sigma_{gausian}$: is the gaussian filter's standard deviation controlling smoothness.

Each component in the final dehazing equation contributes significantly to image quality, and altering their values has a noticeable impact on the outcome. The Gaussian parameter $\sigma_{gausian}$ controls the guided filter, which smooths the transmission map and preserves edges. Removing it results in hazy residue or halo artifacts. Setting $\sigma_{gausian}$ too high can over-smooth the image and decrease detail, while setting it too low may not effectively suppress noise. Gamma correction, controlled by γ_{value}, improves brightness and contrast. Without it, the image may appear dark or faded. A high γ_{value} can provide an unnaturally bright image, while a low value might result in underexposed outputs. CLAHE, $ClipLimit$ and the distribution parameters improve local contrast and detail visibility; eliminating it results in a flat appearance. An extremely high $ClipLimit$ can result in over-enhancement and noise amplification, while a very low number gives minor contrast gains. Experimental results demonstrate that inappropriate adjustment or deletion of any component gives lower PSNR and SSIM scores, as well as inferior visual quality. This demonstrates that each variable makes a considerable contribution to performance, and optimal tuning is required for balanced and successful dehazing.

It is designed to handle both homogeneous and non-homogeneous hazy images, effectively addressing varying haze levels across different regions while preserving image quality and minimizing artifacts. Figure 1 illustrates the systematic flow of the proposed dehazing method, outlining each step from input to final dehazed output.

Figure 1 depicts a step-by-step flowchart for the proposed dehazing technique. It begins by importing the hazy image, which is then checked to ensure that it is in RGB format. If not, the image is transformed to RGB, and the procedure continues. The next stage is pre-processing, which includes resizing and any necessary modifications. The dehazing process is then carried out, followed by a quality validation. If the results are unsatisfactory, the dehazing procedure is revised. Then, post-processing techniques, including guided filtering, gamma correction, and CLAHE, are used. The final stage is to evaluate the output using metrics such as PSNR and SSIM and then produce the dehazed image as the final output.

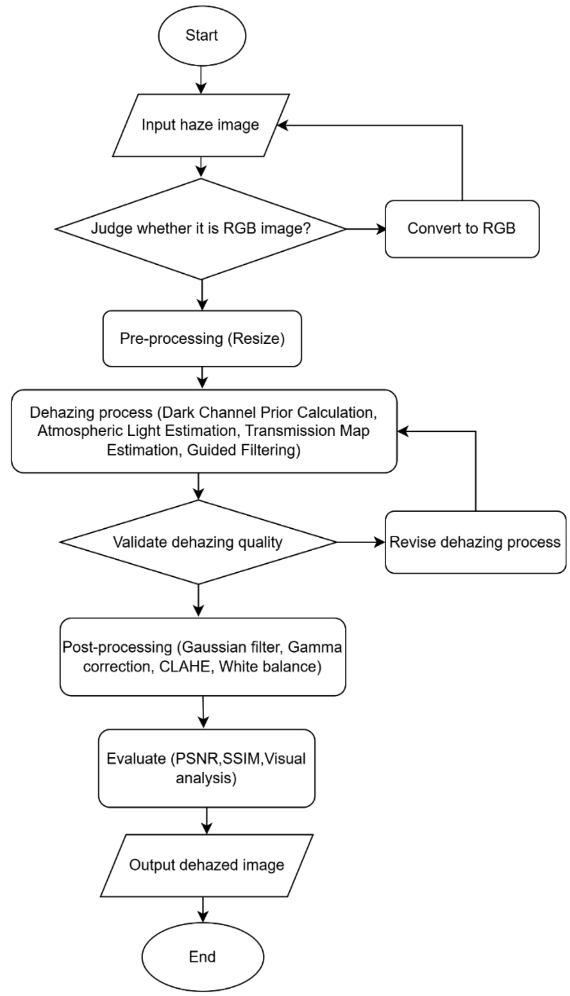

Figure 1. Flowchart of the proposed algorithm.

The flowchart in Figure 1 depicts the phases in the proposed hybrid dehazing method, which combines several essential parameters to optimize image restoration. Patch size (15) is utilized for local dark channel estimation and guided filtering, while $\Omega = 0.95$ determines the degree of haze removal in the transmission map, $\lambda = 0.001$ controls smoothness during guided filtering, while $\gamma = 0.9$ improves brightness and contrast. The Gaussian filter $\sigma = 0.5$ lowers noise, while the resize factor (0.5) speeds up processing. The CLAHE ClipLimit is set to 0.002 for homogeneous haze and 0.02 for non-homogeneous haze, with a uniform distribution to improve contrast.

3. Experiments

3.1 Datasets

RESIDE: A large-scale benchmark for synthetic and real-world hazy images. Used to evaluate dehazing algorithms, including 110,500 synthetic indoor images (ITS) and 313,950 outdoor images (OTS). The RESIDE-Synthetic hazy outdoor Training Set (OTS) was employed in this study to experiment synthesis dataset containing homogeneous haze.

NH-HAZE: A non-homogeneous, realistic dataset containing 55 outdoor hazy images with corresponding haze-free images. The haze was generated using a professional haze machine to simulate real-world conditions. This study explored outdoor homogeneous haze images for experiments

3.2 Implementation Details

The RESIDE and NH-HAZE datasets were used to model both homogeneous and non-homogeneous haze conditions. The RESIDE dataset, which contains hazy images with a consistent haze distribution, was utilized to simulate homogeneous conditions. In contrast, the NH-HAZE dataset, which contains images with non-uniform haze distributions, was used to simulate heterogeneous conditions. Both datasets were analyzed in MATLAB, with haze levels and transmission maps adjusted to exactly match the desired conditions. The hybrid dehazing approach was then implemented in MATLAB. To ensure the reproducibility of the results, the code for this algorithm has been made publicly available on the MATLAB File Exchange community[1].

Starting with atmospheric, which was followed by computing dark channels and refining transmission maps, a scene radiance recovery was then performed. To improve image quality, numerous post-processing techniques were used, such as Gaussian filtering, contrast-limited adaptive Histogram Equalization (CLAHE), gamma correction and white balance adjustment.

3.3 Results

The performance of the proposed hybrid dehazing algorithm was evaluated, focusing on key metrics such as visual quality (qualitative analysis) and PSNR and SSIM (quantitative analysis).

3.3.1 Qualitative analysis

The visual comparison of dehazed images from the proposed hybrid algorithm and state-of-the-art methods provides insight into their effectiveness in handling different haze types. The first column of Figures 1 and 2 represents the original hazy images, while subsequent columns show results from various dehazing techniques. Analysis reveals that some existing methods struggle with haze removal, introducing artifacts or failing to preserve fine details. In contrast, the proposed method achieves superior performance, producing clearer, more detailed images while effectively reducing haze in both homogeneous and non-homogeneous conditions, as shown in Figures 2 and 3.

3.3.2 Quantitative analysis

Quantitative analysis evaluates the performance of the proposed hybrid dehazing algorithm using PSNR and SSIM metrics. Higher PSNR values indicate better image quality with reduced distortion, while higher SSIM values reflect improved structural preservation. The efficiency of the proposed algorithm in improving image quality and preserving structural details is demonstrated by the consistently superior scores it receives when compared to state-of-the-art techniques.

[1] https://www.mathworks.com/matlabcentral/fileexchange/180061-hybrid-dehazing-algorithm-to-enhance-quality-of-hazy-image

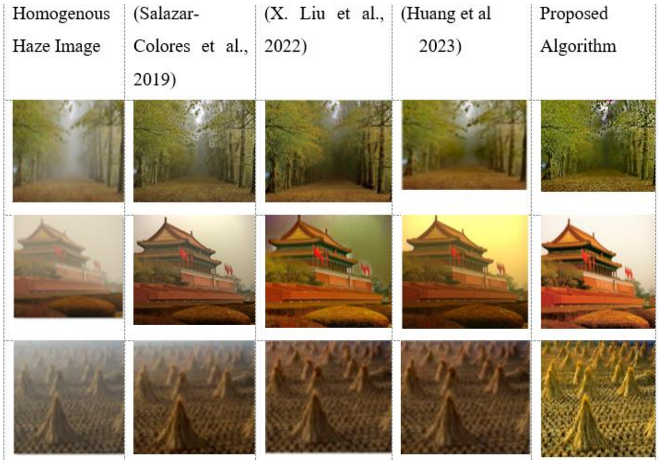

Figure 2. Dehazing algorithms applied to homogeneous haze images.

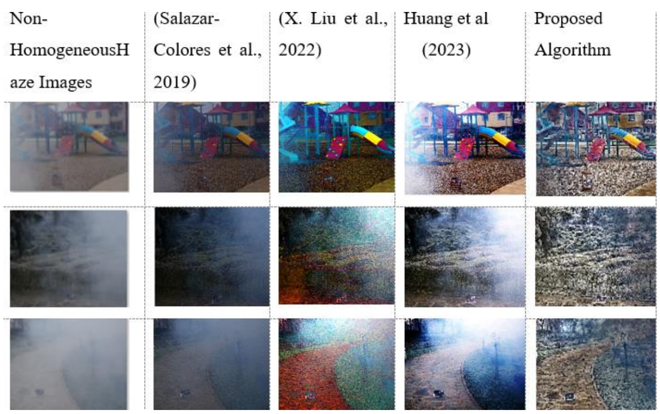

Figure 3. Dehazing algorithms applied to non-homogeneous haze images.

3.3.3 Analysis on PSNR results

The final dehazed images demonstrate that the noise content is minimal compared to the signal content. This improvement was validated using the PSNR. Figure 4 presents the quantitative comparison of dehazing methods based on PSNR values for homogeneous and non-homogeneous images.

A higher PSNR indicates better haze removal and image restoration. The proposed algorithm achieves 35.82 dB for RESIDE outdoor (homogeneous haze) and 17.57 dB for NH-HAZE (non-homogeneous haze), outperforming existing methods.

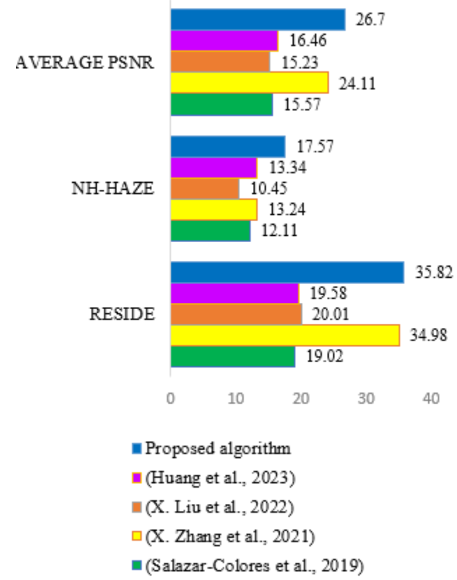

Figure 4. PSNR Values of different dehazing methods.

These results demonstrate its effectiveness in reducing haze while preserving image details and structural integrity, ensuring higher visual fidelity in diverse haze conditions.

3.3.4 Analysis of Structural Similarity Index Measure (SSIM) results

This section analyzes how the proposed method produces a dehazed image that closely resembles the original haze-free image. To validate this, the SSIM was employed.

Figure 5 shows a quantitative comparison of dehazing approaches using SSIM values for homogeneous and non-homogeneous pictures. A greater SSIM suggests improved image quality and structural faithfulness.

The suggested approach achieves SSIM of 0.9800 for RESIDE outside (homogeneous haze) and SSIM of 0.7886 for NH-HAZE (non-homogeneous haze), outperforming previous methods. These findings illustrate its ability to keep image structure while assuring good image restoration under varied hazy situations.

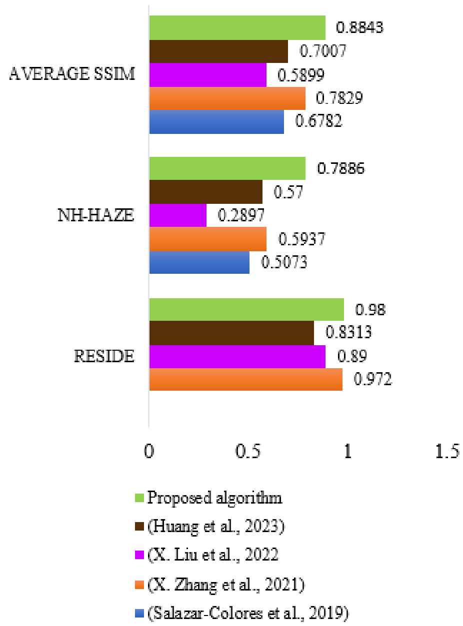

Figure 5. SSIM Values of different dehazing methods.

3.4 Run Time

The proposed dehazing algorithm processes an image in approximately 0.72 seconds, showing competitive runtime efficiency close to the top-performing algorithms (Table 1).

Table 1. Runtime of different dehazing methods.

Algorithm	Salazar et al [15]	Zhang et al [12]	Liu et al [13]	Huang et al [14]	Proposed algorithm
Average Time (s)	0.75	2.01	1.45	0.67	0.72

Although no single algorithm universally outperforms others [16], the proposed algorithm ranks second in speed among the five tested algorithms, achieving an effective balance between speed and dehazing quality, and providing a strong solution among the current methods.

4. Analysis and Discussions

4.1 Analysis

The study shows that the proposed hybrid dehazing algorithm greatly enhances clarity**,** contrast, and colour fidelity, exceeding existing approaches with higher PSNR and SSIM values under both homogeneous and non-homogeneous haze circumstances. The method's strength is in the combination of numerous enhancement techniques, resulting in a versatile and efficient system that balances dehazing effectiveness with processing speed. Importantly, the suggested method's performance was validated not only through controlled trials but also on real-world datasets, NH-HAZE and RESIDE, where it retained superior visual quality and robustness over various haze distributions. This demonstrates its practical relevance to real-time and real-world dehazing applications. Furthermore, the method can be used effectively in real-world scenarios where a reference image is not available, with visual assessment offering a credible indicator of performance. Beyond extending theoretical understanding by resolving gaps in haze removal under various scenarios, the work provides a practical approach for improving image quality in real-world settings. While each enhancement module contributes to overall improvement, future studies incorporating ablation trials could isolate and evaluate their specific effects.

4.2 Generalization capability

The proposed hybrid dehazing algorithm has significant generalization capability by consistently producing high PSNR and SSIM values under both homogeneous and non-homogeneous haze situations, as validated on a variety of datasets including NH-HAZE and RESIDE. Its superiority stems from the strategic combination of physical haze removal and adaptive enhancement techniques, such as guided filtering for edge-preserving refinement, Gaussian filtering for smooth noise suppression, white balance for color distortion correction, gamma correction for brightness enhancement, and CLAHE for local contrast recovery. This carefully crafted combination overcomes the major flaws of traditional approaches, such as over-smoothing, poor color restoration, and loss of detail. As a result, the approach generates visually appealing and structurally precise results while remaining computationally efficient enough for real-time applications. The algorithm's resilience, adaptability, and efficiency distinguish it from existing approaches, as evidenced by both quantitative and visual comparisons.

4.3 Limitations and Challenges

Although the runtime is competitive, the proposed method ranks second in speed among the five tested algorithms due to the added processes required for enhancement. Future works could focus on optimizing computational efficiency by exploring more streamlined mathematical models and faster filtering techniques to further reduce execution time while maintaining image quality.

5. Conclusion

The study presents a hybrid dehazing algorithm demonstrating significant improvements in image quality, particularly in handling homogeneous and non-homogeneous haze conditions. Through comprehensive evaluations using PSNR, SSIM, and visual analysis, the proposed method consistently outperformed several state-of-the-art techniques, offering a robust and versatile solution. The research highlights the algorithm's balance between high-quality dehazing and computational efficiency, making it a valuable contribution to the field of image processing. These findings underscore the potential of the proposed method for various practical applications, from enhancing visibility in weather forecast activities to improving the clarity of images in photography and surveillance.

CONTRIBUTIONS OF CO-AUTHORS

Easter Christopher	[ORCID: 0009-0002-9576-2317]	Conceived the idea, conducted experiments, and wrote the paper
Josiah Nombo	[ORCID: 0000-0002-0020-6936]	Provided technical info on methods and materials, and wrote the paper
Nassor Ally	[ORCID: 0000-0003-4793-7549]	Provided technical info on methods and materials, and wrote the paper

REFERENCES

[1] A. Memarian, T. Laleh, I. Rish, and A. S. Nobandegani, “Is a Good Description Worth a Thousand Pictures? Reducing Multimodal Alignment to Text-Based, Unimodal Alignment,” 2024.

[2] M. Ju, “Imaging-Model-Based Visibility Recovery for Single Hazy Images,” no. September, 2020.

[3] S. C. Agrawal and A. S. Jalal, *A Comprehensive Review on Analysis and Implementation of Recent Image Dehazing Methods*, vol. 29, no. 7. Springer Netherlands, 2022. doi: 10.1007/s11831-022-09755-2.

[4] S. Singh, M. T. Scholar, and C. Engineering, “A Review of Image Dehazing Techniques Using Dark Channel,” vol. 10, no. 8, pp. 743–746, 2023.

[5] X. Liu, H. Li, and C. Zhu, “Joint Contrast Enhancement and Exposure Fusion for,” *IEEE Trans. Multimed.*, vol. 24, pp. 3934–3946, 2022, doi: 10.1109/TMM.2021.3110483.

[6] F. Guo, J. Yang, Z. Liu, and J. Tang, “Haze removal for single image: A comprehensive review,” *Neurocomputing*, vol. 537. pp. 85–109, 2023. doi: 10.1016/j.neucom.2023.03.061.

[7] V. Varshney, “Single Image Haze Removal Techniques Based on Priors, Fusion and Deep Learning: A Comprehensive Survey,” 2023.

[8] J. L. Lisani and C. Hessel, “Dehazing with Dark Channel Prior: Analysis and Implementation,” *Image Process. Line*, vol. 14, pp. 173–193, 2024, doi: 10.5201/ipol.2024.530.

[9] K. He, J. Sun, and X. TTang, “Single image haze removal using dark channel prior,” *2009 IEEE Conf. Comput. Vis. Pattern Recognition, CVPR 2009*, no. January 2011, pp. 1956–1963, 2010, doi: 10.1109/CVPRW.2009.5206515.

[10] S. Lee, S. Yun, J. H. Nam, C. S. Won, and S. W. Jung, “A review on dark channel prior based image dehazing algorithms,” *Eurasip J. Image Video Process.*, vol. 2016, no. 1, pp. 1–23, 2016, doi: 10.1186/s13640-016-0104-y.

[11] F. Guo, J. Yang, Z. Liu, and J. Tang, “Haze removal for single image: A comprehensive review,” *Neurocomputing*, vol. 537, pp. 85–109, 2023, doi: 10.1016/j.neucom.2023.03.061.

[12] X. Zhang, J. Wang, T. Wang, and R. Jiang, “Hierarchical Feature Fusion with Mixed Convolution Attention for Single Image Dehazing,” vol. 8215, no. c, pp. 1–13, 2021, doi: 10.1109/TCSVT.2021.3067062.

[13] X. Liu, H. Li, and C. Zhu, “Joint Contrast Enhancement and Exposure Fusion for Real-World Image Dehazing,” *IEEE Trans. Multimed.*, vol. 24, pp. 3934–3946, 2022, doi: 10.1109/TMM.2021.3110483.

[14] S. Huang, Y. Zhang, and O. Zhang, “Image Haze Removal Method Based on Histogram Gradient Feature Guidance,” *Int. J. Environ. Res. Public Health*, vol. 20, no. 4, 2023, doi: 10.3390/ijerph20043030.

[15] S. Salazar-Colores, J. M. Ramos-Arreguín, J. C. Pedraza-Ortega, and J. Rodríguez-Reséndiz, “Efficient single image dehazing by modifying the dark channel prior,” *Eurasip J. Image Video Process.*, vol. 2019, no. 1, 2019, doi: 10.1186/s13640-019-0447-2.

[16] D. H. Wolpert, “What is important about the No Free Lunch theorems?” pp. 1–15, 2020.

[17] Y. Zhou, Z. Chen, B. Sheng, J. Kim, and E. Wu, “AFF-Dehazing: Attention-based feature fusion network for low-light image Dehazing,” no. April, pp. 1–12, 2021, doi: 10.1002/cav.2011.